Vol. 21, No. 2(2022) Mat2619
Revista Mexicana de Ingeniería Química

Electrochemical evaluation of conjugated oligophenylenimine in aqueous medium for bandgap determination

Evaluación electroquímica de una oligofenilenimina conjugada en medio acuoso para la determinación de bandgap

M.A. Amado-Briseño[1], C. Cortés-López[1], R.A. Vázquez-García[1], V.E. Reyes-Cruz[1*], G. Urbano-Reyes[1], A. Trujillo-Estrada[2], A. Espinosa-Roa[3]

[1]*Área Académica de Ciencias de la Tierra y Materiales, Universidad Autónoma del Estado de Hidalgo, Mineral de la Reforma, Hidalgo, México.*

[2]*CONACYT - Consejo Nacional de Ciencia y Tecnología, Depto. de Cátedras, Av. Insurgentes Sur 1582, Col. Crédito constructor, Deleg. Benito Juárez, Ciudad de México, CP. 03940, México.*

[3]*CONACYT-Centro de Investigación en Química Aplicada, Parque de Innovación e Investigación Tecnológica (PIIT), Apodaca, NL, Mexico.*

Received: October 5, 2021; Accepted: April 28, 2022

Abstract

In the present work, three aqueous medium were used: sodium acetate ($NaC_2H_3O_2$), potassium nitrate (KNO_3) and sodium nitrate ($NaNO_3$) at two different scanning speeds, 50 and 100 mVs^{-1}, to evaluate the bandgap of the conjugated oligophenylenimine called DAFCHO by cyclic voltammetry (CV). DAFCHO was synthesized by solid-phase mechanosynthesis from 2, 7-diaminofluorene and 2, 5-bis(octyloxy)terephthalaldehyde and deposited as a film in a configuration a) glass/ITO (indium tin oxide)/DAFCHO and b) glass. The results showed an electrochemical bandgap range of 2.39 to 2.47 eV at 50 mVs^{-1} and from 2.59 to 2.68 eV at 100 mVs^{-1} on glass/ITO/DAFCHO. While the electrochemical bandgap on glass/DAFCHO in range of 2.58 to 2.64 eV at 50 mVs^{-1}; which are close to the optical bandgap and electrochemical bandgap of 2.56 eV and 2.35 eV reported in the literature, calculated by UV-vis absorption spectroscopy in solution acetonitrile (ACN) and electrochemically in a BU_4NPF_6/ACN electrolyte. In addition, a greater degradation of the film of the organic compound DAFCHO was observed in the three aqueous medium ($NaC_2H_3O_2$, KNO_3 and $NaNO_3$), compared with the anhydrous medium (BU_4NPF_6/ACN) from the literature. On the other hand, the electrical evaluation of semiconductor DAFCHO in an electronic device exhibits the characteristic behaviour of a P-N-type junction diode.

Keywords: mechanosynthesis, oligophenylenimine, cyclic voltammetry, organic semiconductor, diode.

Resumen

En el presente trabajo se utilizan tres medios acuosos: acetato de sodio ($NaC_2H_3O_2$), nitrato de potasio (KNO_3) y nitrato de sodio ($NaNO_3$) a dos velocidades de barrido diferentes, 50 y 100 mVs^{-1} para evaluar la banda prohibida de la oligofenilenimina conjugada denominada DAFCHO por voltamperometría cíclica (CV, por sus siglas en inglés). El DAFCHO se sintetizó mediante mecanosíntesis en fase sólida a partir de: 2,7-diaminofluoreno y 2, 5-bis (octiloxi)tereftalaldehído y se depositó como una película en una configuración a) vidrio/ITO (óxido de indio estaño)/DAFCHO y b) vidrio/DAFCHO. Los resultados mostraron un rango de banda prohibida electroquímica de 2.39 a 2.47 eV a 50 mVs^{-1} y de 2.59 a 2.68 eV a 100 mVs^{-1} sobre vidrio/ITO/DAFCHO. Mientras que el bandgap electroquímico en vidrio/DAFCHO está en el rango de 2,58 a 2,64 eV a 50 mVs^{-1}; que están cerca de la bandgap óptico y bandgap electroquímico of 2.56 eV and 2.35 eV reportados en la literatura, calculado por espectroscopia de absorción UV-vis en solución de acetonitrilo (ACN) y electroquímicamente en un electrolito de BU_4NPF_6/ACN. Además, se mostró una mayor degradación de la película del compuesto orgánico DAFCHO en los tres medios acuosos ($NaC_2H_3O_2$, KNO_3 y $NaNO_3$), en comparación con el medio anhidro (BU_4NPF_6/ACN) de la literatura. Por otro lado, la evaluación eléctrica del semiconductor DAFCHO en un dispositivo electrónico exhibe un comportamiento similar al de un diodo de unión tipo P-N.

Palabras clave: mecanosíntesis, oligofenilenimina, voltametría cíclica, semiconductor orgánico, diodo.

* *Corresponding author. E-mail*: reyescruz16@yahoo.com

https://doi.org/10.24275/rmiq/Mat2619
ISSN:1665-2738, *issn-e*: 2395-8472

1 Introduction

Conjugated oligophenylenimines are low molecular weight organic molecules that may contain polycyclic aromatic groups (naphthalene, anthracene, fluorene, etc.) in their structure, have semiconductor properties, and can be used in the manufacture of some organic optoelectronic devices, such as OLEDs (Amado-Briseño *et al*., 2022; Bernal *et al*., 2021), solar cells (Espinosa-Roa *et al*., 2019; Arrieta-Almario *et al*., 2020; Duan & Uddin, 2020) and smart windows (Ke *et al*., 2019; Jia *et al*., 2021). Among the methods of obtaining oligophenylenimines, the mechanosynthesis technique has the advantage of reducing the time of conjugated compound synthesis and obtaining better results than traditional synthesis methods (Pérez *et al*., 2015).

There are different types of methods used for the calculation of the optical bandgap of organic semiconductors, among them are:

UV-Vis spectroscopy, this method is employed for samples in solution using quartz cells, solid samples using a sample holder with a quartz window and film samples deposited on quartz substrates; the calculation of the optical bandgap is performed through the tangent from the maximum peak of the absorption spectrum to the X-axis cut-off that spans most of the points on the edge of the spectrum to where the spectrum ends. The determined bandgap values for this method are in the range of 1.5 eV to 3 eV. This is an inexact but functional method (Mejía-Hernández *et al*., 2021; Flores-Noria *et al*., 2014).

Diffuse Reflectance Spectroscopy (DRS with integrated sphere) this method uses the Kubelka-Munk function, in this method a quartz cell is used where the powdered sample is introduced, an adequate amount of the organic semiconductor is required to fill the cell, which represents a disadvantage to the method (Ensayos-Mediumnte-Uv-Vis @ www.labte.es, n.d.). This technique allows us to obtain optical bandgap values in the range 1.67 eV to 2.13 eV (Yahia *et al*., 2016).

X-Ray Photoelectron Spectroscopy (XPS) by means of this technique, it is possible to calculate the electrical properties using powders and films such as valence band and Fermi levels (Xps @ www.scai.uma.es, n.d.); using this technique the literature report value of bandgap of 1.63 eV (Schlaf *et al*., 1999). The samples to be analyzed can be: thin films or sheets, compact solids, gems, archaeological material, crystals, suspensions. This equipment is expensive due to the large amount of information obtained, such as electrical properties, morphological properties, masses, etc.

Through cyclic voltammetry, the electrochemical bandgap has been calculated for organic semiconductor materials in non-aqueous electrolyte solutions as ACN and on films deposited in glass/ITO; reporting values in the range of 2.35 a 2.66 eV (Li *et al*., 2004), (Flores-Noria *et al*., 2014). The use of organic solvents represents a disadvantage for the method because it increases costs, can be toxic and difficult to evaporate, and the electrolytes of phosphate salts and organic perchlorates are expensive and toxic.

In this sense the CV technique has proven to be an efficient tool (Chooto, 2019; Sandford *et al*., 2019) to determine the electrochemical bandgap of organic compounds, as it describes the electronic transitions that occur during the excitation of the valence electrons of the conjugated molecule. In the research that precedes this paper is, the potentials determined in the redox processes for oligophenylenimine (DAFCHO, obtained for the mechanosynthesis technique) on glass/ITO in a BU_4NPF_6/ACN electrolyte gives an electrochemical bandgap value of 2.35 eV (Amado-Briseño *et al*., 2019). However, thus far, there have been not studies on the evaluation of the electrochemical bandgap of organic molecules in aqueous medium and substrate relatively more economical; such as the use of aqueous medium and the deposition of the organic semiconductor on glass substrates without ITO; that allows to eliminate the disadvantage for of obtained the electrochemical bandgap of organic compounds.

In the present work, a conjugated oligophenylenimine (DAFCHO) carrying fluorene groups (Saeed *et al*., 2021; Banerjee *et al*., 2021; Noirbent *et al*., 2021; Amado-Briseño *et al*., 2019) was synthesized by solid phase mechanosynthesis and deposited as a film in a configuration glass/ITO/DAFCHO and glass/DAFCHO, to evaluate and determine their respective electrochemical bandgap in three electrolytic aqueous medium ($NaC_2H_3O_2$, KNO_3 and $NaNO_3$) and compare them with the optical bandgaps in solution and film of DAFCHO. For this, the redox potentials were obtained using CV, along with the HOMO-LUMO levels at scanning speeds of 50 mVs^{-1} and 100 mVs^{-1}.

2 Experimental

2.1 Electrochemical system

A typical three-electrode cell was used, where the working electrode was the conjugated oligophenylenimine (DAFCHO), which was deposited on glass/ITO and glass by using the self-assembly technique (Ramos *et al*., 2020). A saturated calomel electrode (SCE) was used as the reference electrode, and a platinum wire was used as the counter electrode. The behaviour of oligophenylenimine was evaluated in four electrolytic medium: 0.1-M BU_4NPF_6 diluted in acetonitrile (ACN) and $NaC_2H_3O_2$, KNO_3 and $NaNO_3$ diluted in deionized water (DIH_2O). The reagents used were of analytical grade and were purchased from Sigma-Aldrich (USA), while the solvents used were purchased from J.T. Baker (USA). Note that BU_4NFP6/ACN was used as the comparative supporting electrolyte (M. A. Amado-Briseño *et al*., 2019) for the calculated electrochemical bandgap value in the electrolytic medium with a deionized water solvent. These solutions are support electrolytes that favor the redox responses in solution or film (Isa *et al*., 2012) and decrease mass transport by migration. The redox responses of these K, Na and NO ions occurs at more negative potentials and positive, allowing observed the redox processes of the organic compound DAFCHO.

Voltammetric measurements were carried out in the cathodic direction in the potential range of -2 V to 2 V vs. SCE, with scanning speeds of 50 mVs^{-1} and 100 mVs^{-1} at room temperature and by deoxygenating each supporting electrolyte with nitrogen (high purity) for 30 min. CV measurements were performed using a Princeton Applied Research potentiostat/galvanostat with the Power Suite Software interface provided by the same company. While the electrochemical impedance measurements on glass/ DAFCHO were carried in three aqueous medium sodium acetate ($NaC_2H_3O_2$), potassium nitrate (KNO_3) and sodium nitrate ($NaNO_3$) in order to review the conductive character of the DAFCHO. The impedances measurements were performed using an AutoLap potentiostat/galvanostat from 0.1 Hz to 10 KHz.

2.2 Oligophenylenimine electrode preparation

Working electrodes were prepared using the self-assembly technique with a solution of 5-mg conjugated compound DAFCHO diluted in 10-mL chloroform. Then, the glass/ITO and the glass was immersed for 15 min in the mentioned solution and dried in open air. The process was repeated thrice to form layers of the conjugated compound DAFCHO on the glass/ITO and glass, while the covered surface with the compound measured 2 cm × 1 cm. The electrochemical bandgap (Eg(EC)) was calculated using the oxidation and reduction potentials (Eq. 1). The HOMO and LUMO values were estimated with these potential values, according to Eqs. 2 and 3, using as internal standard the ferrocene energy level in a vacuum equivalent to 4.4 eV (Sweety *et al*., 2019).

$$Eg_{(EC)} = LUMO - HOMO \quad (1)$$

$$HOMO = -(E_{ox} + 4.4eV) \quad (2)$$

$$LUMO = -(E_{red} + 4.4eV) \quad (3)$$

2.3 Electrical measurement

An electrical measurement to determine the current-voltage behaviour in an electronic device configuration glass/ITO/PEDOT:PSS (poly(3,4-ethyldioxythiophene)-poly(styrenesulfonate)) /DAFCHO/Al was conducted over a range of 0 to 6.5 V in direct polarisation at room temperature, using an Agilent 4155C semiconductor parameter analyser.

2.4 Optical characterization on quartz/DAFCHO

Optical absorption characterization in film of the oligophenylenimine was carried out using a Perkin-Elmer Lambda XLS UV-Vis to determine the transitions $\pi - \pi^*$. The film of quartz/DAFCHO formed for this study were generated in the same way as mentioned above. Meanwhile, with obtained values from the absorption spectra of the oligophenylenimine the optical band gap $Eg_{(Opt)}$ was calculated, using Eq. 4 (Vazquez *et al*., 2020).

$$Eg_{(Opt)} = hc/\lambda \quad (4)$$

2.5 X ray diffraction (DRX) on glass/ITO/DAFCHO

XRD was carried out on the glass, glass/DAFCHO, glass/ITO/DAFCHO without degraded and when was electrochemically degraded in BU_4NPF_6/ACN and three aqueous supporting electrolytes ($NaC_2H_3O_2$, KNO_3 and $NaNO_3$), using an Equinox 2000 X-ray diffractometer (Inel), which uses a monochromaticCoKα radiation (λ = 1.789 Å),

produced at 30 kV and 20 mA. Measurements to identify the species presents were carried in a window from 5º to 110º in 2θ with increments of 0.20 in a time of 30 min.

3 Results and discussion

3.1 *Electrochemical analysis of oligophenylenimine*

Figures 1a, 1b, 1c and 1d show the glass/ITO/DAFCHO voltammograms (black line) initiated in the cathodic direction for the BU_4NPF_6/ACN, $NaC_2H_3O_2$, KNO_3 and $NaNO_3$ electrolytic mediums at the scanning speed of 50 mVs^{-1} in the potential range of -2 V to 2 V vs. SCE. Figures 1a and 1b show that the voltammograms obtained in the BU_4NPF_6/ACN and $NaC_2H_3O_2$ electrolytic medium exhibit a reduction process at -1.26 V and -1.20 V, respectively (see insets of Figures 1a and 1b), followed by an increase in the cathodic current attributed to the hydrogen evolution process. While the voltammograms obtained in the KNO_3 and $NaNO_3$ electrolytic medium (Figures 1c and 1d, respectively), reveal that the first reduction process began at the relatively low cathodic potential of -1.15 V and -1.08 V, respectively (see insets), followed by a greater increase in the cathodic current, a characteristic of nitrate salt electrolytes (Broder *et al.*, 2007; Abbas *et al.*, 2019). Therefore, the first reduction process observed in the four electrolytic mediums could be attributed to an electron gain of the conjugate compound at the LUMO energy level. Because, the voltammetric response of the glass/ITO (red line) does not present reduction processes in the potential range from -1 to -1.3 V in the four medium.

By reversing scanning to anodic potentials, we observed that when using the BU_4NPF_6/ACN supporting electrolyte, there was a single oxidation peak before the oxygen evolution at 1.07 V (see inset of Figure 1a). In contrast, in the case of the $NaC_2H_3O_2$ supporting electrolyte, two oxidation peaks were observed before the oxygen evolution at -1.01 V and 1.27 V (see insets of Figure 1b).

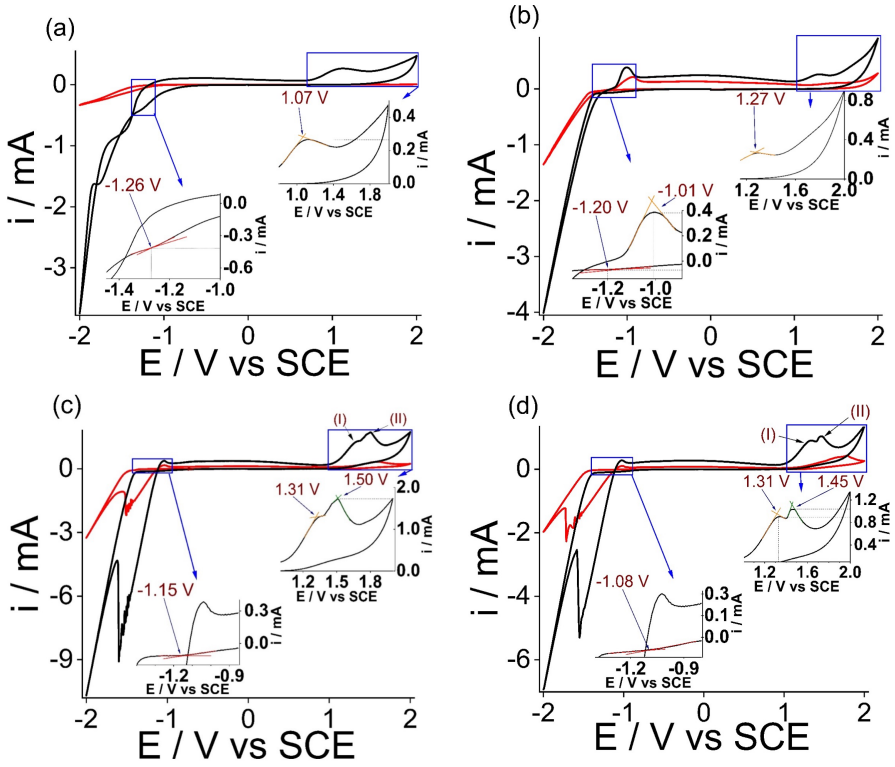

Fig. 1 Cyclic voltammetries for glass/ITO/DAFCHO (black line) and glass/ITO (red line) in systems (a) BU_4NPF_6, (b) $NaC_2H_3O_2$, (c) KNO_3, (d) $NaNO_3$, from -2 to 2V vs SCE with a scanning speed of 50 mVs^{-1}.

Table I. Electrochemical bandgap calculated for each electrolyte at a scanning speeds of 50 mVs-1 obtained in glass/ITO/DAFCHO.

System	$E_{(Red)}$	$E_{(Ox)}$	LUMO	HOMO	$Eg_{(EC)}$
BU_4NPF_6/ACN	-	-	-	-	*2.35
$NaC_2H_3O_2$/DIH_2O	-1.2	1.27	-3.2	-5.67	2.47
KNO_3/DIH_2O	-1.08	1.31	-3.32	-5.71	2.39
$NaNO_3$/DIH_2O	-1.15	1.31	-3.25	-5.71	2.46

*(Amado-Briseño *et al*., 2019)

The last peak was attributed to the electron evolution reaction of the conjugated compound DAFCHO, since in the potential range of 0.9 V at 1.3 V, the voltammetric response of glass/ITO (red line of figure 1a and 1b) does not present oxidation processes attributed to ITO or the supporting electrolyte. This process of the second oxidation peak in glass/ITO/DAFCHO occurred under the conditions of high oxidative stress typical of the formation of polarons, which involved the detachment of an electron from the conjugated compound and its interaction with the crystal lattice (Flores-Noria *et al*., 2014).

In contrast, in the KNO_3 and $NaNO_3$ electrolytic medium, two well-differentiated oxidation processes of the conjugated compound DAFCHO were observed. The first oxidation process (I) occurred for both medium at a potential of 1.31 V (see insets of Figures 1c and 1d), while the second oxidation process (II) was observed at potentials of 1.50 V and 1.45 V, respectively (see insets of Figures 1c and 1d). This second oxidation process could be attributed to the loss of the electrons from the conjugated compound at the HOMO energy level; since in the potential range of 0.9 V at 1.3 V, the voltammetric response of glass/ITO (red line of figure 1c and 1d) does not present oxidation processes attributed to ITO or the supporting electrolyte.

According to the values obtained from the $Eg_{(EC)}$ (electrochemical bandgap) calculation with Eqs. 1-3 (see Table I), the $NaC_2H_3O_2$/DIH_2O, KNO_3/DIH_2O and $NaNO_3$/DIH_2O systems presented values of 2.47 eV, 2.39 eV and 2.46 eV, respectively, which were close to the 2.35 eV value reported for the BU_4NPF_6/ACN system (M. A. Amado-Briseño *et al*., 2019). This suggested that the conjugated compound DAFCHO was located within the bandgap range of organic semiconductor materials (Dinesh Pathak *et al*., 2021). Note that the DAFCHO compound film underwent significant surface degradation when it interacted with the four electrolytic medium. However, this degradation was greater in $NaC_2H_3O_2$, KNO_3 and $NaNO_3$, which could be attributed to the nature of the medium and their interaction with the film.

In order to evaluate whether the potentials values in the redox processes of the conjugated compound DAFCHO have not limited by the mass transfer and remained constant with the film degradation or whether this degradation significantly increased the electric resistance, CV were carried out at a higher scanning speed (100 mVs^{-1}) in the four electrolytic medium. Figures 2a, 2b, 2c and 2d show the glass/ITO (line red) and glass/ITO conjugated compound DAFCHO (line black) voltammograms initiated in the cathodic direction for the BU_4NPF_6 (diluted in acetonitrile), $NaC_2H_3O_2$, KNO_3 and $NaNO_3$ (diluted in deionized water) electrolytic medium at the scanning speed of 100 mVs^{-1}, in the potential range of -2 V to 2 V.

The voltammetries of Figure 2 show that, as at the speed of 50 mVs^{-1}, the voltamperometric responses of the glass/ITO in the 4 medium in study at 100 mVs^{-1} (red lines) do not present redox processes in the potentials where the DAFCHO have redox response.

In addition, it is appreciated that the conjugated compound DAFCHO reduction and oxidation processes with an irreversible-type kinetic behaviour, including a process corresponding to the formation of polarons. The redox processes of the DAFCHO compound are in the same potential range at both scanning speeds, indicating that it is not limited by the mass transfer process since the species that react are on the surface of the electrode. In the BU_4NPF_6/can supporting electrolyte, there was a shift in the DAFCHO reduction process toward a less cathodic potential of -1.09 V (see inset of Figure 2a) with respect to that observed in the CV at 50 mVs^{-1}. Moreover, in the cases of the $NaC_2H_3O_2$, KNO_3 and

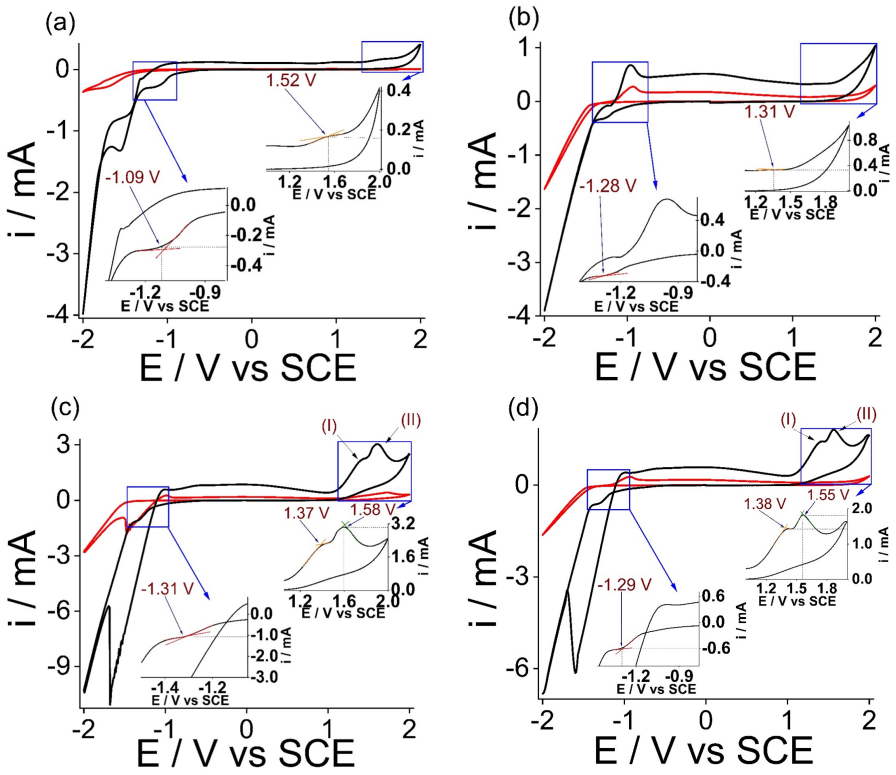

Fig. 2 Cyclic voltammetries for glass/ITO/DAFCHO (black line) and glass/ITO (red line) in systems (a) BU_4NPF_6, (b) $NaC_2H_3O_2$, (c) KNO_3, (d) $NaNO_3$, from -2 to 2V vs SCE with a scanning speed of 100 mVs^{-1}.

$NaNO_3$ electrolytic medium, the reduction process appeared to have a higher cathodic potential (-1.28 V, -1.31 V and -1.29 V, respectively; see insets of Figures 2b, 2c and 2d) than that observed in the CV at 50 mVs^{-1}.

Furthermore, in the BU_4NPF_6/can supporting electrolyte, a lower cathodic current of -0.258 mA (see inset of Figure 2a) corresponding to the DAFCHO reduction peak was observed with respect to the scanning at 50 mVs^{-1} of -0.4 mA (see inset of Figure 1a). However, in the cases of the $NaC_2H_3O_2$, KNO_3 and $NaNO_3$ electrolytic medium, higher cathodic currents were observed at 100 mVs^{-1} (-0.32 mA, -1.06 mA and -0.577 mA, respectively; see insets of Figures 2b, 2c and 2d) than at the scanning speed of 50 mVs^{-1} (-0.068 mA, -0.112 mA and -0.071 mA, respectively; see insets of Figures 1b, 1c and 1d). The more negative potentials and increased cathodic current in the reduction processes with the $NaC_2H_3O_2$, KNO_3 and $NaNO_3$ electrolytic medium could be attributed to the superficial modification produced by the previous oxidation or degradation of the DAFCHO film in the voltammetries conducted at the scanning speed of 50 mVs^{-1}.

By reversing the potential sweep, we observed that the oxidation peak of the conjugated compound DAFCHO in the BU_4NPF_6/ACN, $NaC_2H_3O_2$, KNO_3 and $NaNO_3$ medium presented more positive potential values (1.52 V, 1.31 V vs. SCE; 1.37 V, 1.58 V; 1.38 V and 1.55 V; see insets of Figures 2a, 2b, 2c and 2d, respectively) than those obtained in the CV conducted at 50 mVs^{-1} (1.07 V, 1.27 V; 1.31 V, 1.50 V; 1.3 V and 1.45 V; see insets of Figures 1a, 1b, 1c and 1d, respectively). This behaviour in the displacement at the more positive potentials of the oxidation peaks of the conjugated compound (DAFCHO) in the four electrolytic medium was attributed to the superficial modification produced by the previous oxidation or degradation of the oligophenylenimine film.

In contrast, in the BU_4NPF_6/ACN medium, there was a lower anodic current of 0.164 mA from the process corresponding to the oxidation peak of the conjugated compound DAFCHO, when the scanning was performed at 100 mVs^{-1} (see inset of Figure 2a) than that obtained at 50 mVs^{-1} (0.26 mA) (see inset of Figure 1a). However, in the cases of the $NaC_2H_3O_2$, KNO_3 and $NaNO_3$ electrolytic medium, we observed higher anodic currents

Table II. Electrochemical bandgap calculated for each electrolyte at a scanning speeds of 100 mVs-1 glass/ITO/DAFCHO.

System	$E_{(Red)}$	$E_{(Ox)}$	LUMO	HOMO	$Eg_{(EC)}$
BU_4NPF_6/ACN	-1.09	1.52	-3.31	-5.92	2.61
$NaC_2H_3O_2$/DIH_2O	-1.28	1.31	-3.12	-5.71	2.59
KNO_3/DIH_2O	-1.31	1.37	-3.09	-5.77	2.68
$NaNO_3$/DIH_2O	-1.29	1.38	-3.11	-5.78	2.67

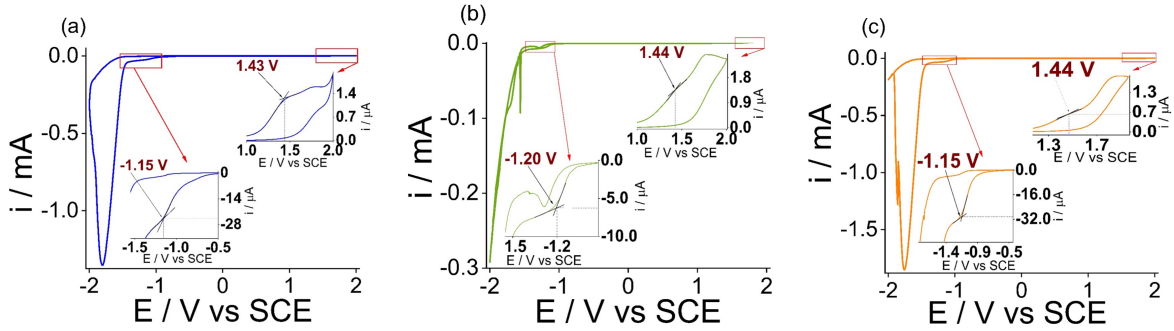

Fig. 3 Cyclic voltammetries for glass/DAFCHO in systems (a) $NaC_2H_3O_2$, (b) KNO_3, (c) $NaNO_3$, from -2 to 2V vs SCE with a scanning speed of 50 mVs^{-1}.

(0.331 mA, 2.06 mA and 1.40 mA, respectively; see insets of Figures 2b, 2c and 2d) on the oxidation process of the conjugated compound DAFCHO at 100 mVs^{-1}, than those obtained at 50 mVs^{-1} (0.26 mA, 1.24 mA and 0.90 mA, respectively; see insets of Figures 1b, 1c and 1d). The increase in the anodic current in the $NaC_2H_3O_2$, KNO_3 and $NaNO_3$ electrolytic medium indicated that the oxidation processes at 100 mVs^{-1} were due to the conjugated compound, which being on the surface, was not limited to the diffusion processes of the oxidised species.

In addition, we observed that the interaction of polarons with a crystal lattice was greater by applying an increase in the scanning speed (100 mVs^{-1}), because of the greater deformation of the crystal lattice that surrounded the polaron (Flores-Noria *et al*., 2014), which made their mobility more efficient. Note that the previous modification of the surface could contribute to a deterioration of the conditions of oxidative stress, affecting the mobility of the electrons.

Moreover, an increase in the electrochemical bandgap $Eg_{(EC)}$ was observed in the BU_4NPF_6/ACN, $NaC_2H_3O_2$/DIH_2O, KNO_3/DIH_2O and $NaNO_3$/DIH_2O systems at 100 mVs^{-1} (2.61 eV, 2.59 eV, 2.68 eV and 2.67 eV, respectively; see Table II), as compared to that at 50 mVs^{-1} (2.35 eV, 2.47 eV, 2.39 eV and 2.46 eV, respectively; see Table I). The electrochemical bandgap at 50 mVs^{-1} and 100 mVs^{-1} increased in increments of 0.12 and 0.33 eV, respectively. This increase was attributed to the previous oxidation suffered by the films in the first scanning. However, we observed that the conjugated compound DAFCHO retained its properties as a semiconductor material by having an electrochemical bandgap of less than 3 eV. The results confirmed that these values were acceptable for this compound type, i.e. for organic semiconductor materials (Dinesh Pathak *et al*., 2021).

In order to determine the response of the conjugated compound DAFCHO in a more accessible substrate to calculate the electrochemical bandgap, voltammetric studies of the compound on glass (glass/DAFCHO) in aqueous medium are carried out.

Figures 3a, 3b and 3c show the glass/DAFCHO voltammograms initiated in the cathodic direction for $NaC_2H_3O_2$, KNO_3 and $NaNO_3$ supporting electrolytes at the scanning speed of 50 mVs^{-1} in the potential range of -2 V to 2 V. Figure 3 show that the voltammograms obtained in $NaC_2H_3O_2$ supporting electrolyte present the reduction and oxidation process of the DAFCHO at -1.15 V and 1.43 V respectively (see insets of Figures 3a). While the voltammograms obtained in the KNO_3 and $NaNO_3$ supporting electrolytes, present the reduction and oxidation process of the DAFCHO at -1.2 V and 1.44 V (see insets of Figure 3b) and -1.15 V and 1.44 V (see insets of Figure 3c), respectively.

Table III. Electrochemical bandgap calculated for each electrolyte at a scanning speeds of 50 mVs-1; obtained in glass/DAFCHO.

System	E(Red)	E(Ox)	LUMO	HOMO	Eg(EC)
$NaC2H_3O_2/DIH_2O$	-1.15	1.43	-3.3	-5.8	2.58
KNO_3/DIH_2O	-1.2	1.44	-3.2	-5.8	2.64
$NaNO_3/DIH_2O$	-1.15	1.44	-3.3	-5.8	2.59

The Table III show the values obtained from the Eg(EC) (electrochemical bandgap) calculation with Eqs. 1-3 using the potentials of the voltammograms of figure 3 in the $NaC_2H_3O_2/DIH_2O$, KNO_3/DIH_2O and $NaNO_3/DIH_2O$ systems.

In the Table III was observed an increase in the electrochemical bandgap $Eg_{(EC)}$ when using glass/DAFCHO of 2.58 eV, 2.64 eV and 2.59 eV in the $NaC_2H_3O_2/DIH_2O$, KNO_3/DIH_2O and $NaNO_3/DIH_2O$ systems respectively at 50 mVs^{-1}, as compared to that at 50 mVs^{-1} of glass/ITO/ DAFCHO of 2.47 eV, 2.39 eV and 2.46 eV, respectively (see Table I).

This values of the electrochemical bandgap Eg(EC) obtained in glass/DAFCHO presented an acceptable difference when compared with the optical bandgap in solution and the electrochemical bandgap on glass/ITO/DAFCHO in BU_4NPF_6/ACN supporting electrolyte reported in the literature (2.56 eV and 2.35 eV, respectively; Amado-Briseño *et al*., 2019). Thus, it was determined that the evaluated electrolytic aqueous medium could be used to calculate the electrochemical bandgap of the conjugated compound DAFCHO on glass.

3.2 Optical band gap determination on quartz/DAFCHO

The conjugate compound DAFCHO study of the optical band gap was carried out through its UV-Vis spectrum on *quartz*. In Figure 4 is observed that the maximum peak for DAFCHO have a value of 465 nm that corresponds to the $\pi - \pi^*$ transitions.

The calculated optical bandgap in film (quartz/ DAFCHO) whit the Eq. 4 (M. A. Amado-Briseño *et al*., 2019) was 2.34 eV; which is close to that calculated on glass/ITO/DAFCHO in BU_4NPF_6/ACN supporting electrolyte reported in the literature. This presented an acceptable difference when compared to the electrochemical band gap obtained in glass/DAFCHO and glass/ITO/DAFCHO at 50 $mV.s^{-1}$.

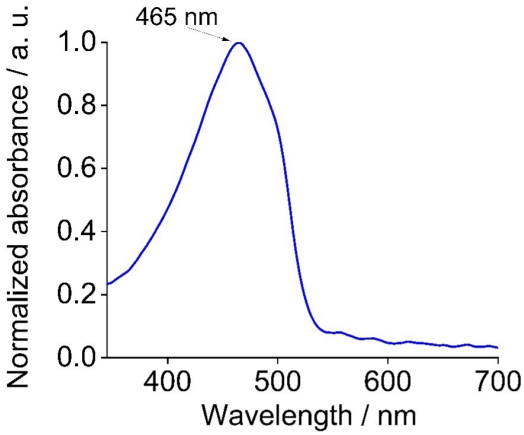

Fig. 4 Absorption spectra of quartz/DAFCHO.

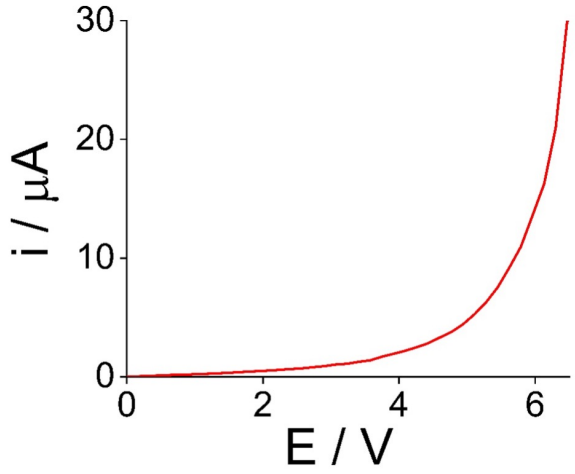

Fig. 5 Current-Voltage curve of electronic device (glass/ITO/PEDOT:PSS/DAFCHO/Al)

3.3 Electrical characterization of an electronic device glass/DAFCHO

Figure 5 shows the current-voltage curve of the DAFCHO device, which exhibited an exponential growth of the current in the case of direct polarisation. Although, in the range of 0 to 3.25 V, ohmic behaviour was observed in the chart along with a significant increase in the current, which showed the

electronic mobility present in the device. Therefore, the DAFCHO device was found to behave like a P-N-type junction diode to low voltages (Saive, 2019; Rau & Kirchartz, 2019).

In order to determine the conductive characteristic of the compound DAFCHO, impedance studies are carried out in the 3 aqueous medium.

3.4 Electrochemical impedance on glass/DAFCHO

Figure 6 shows the Nyquist diagrams obtained on the glass/ITO/DAFCHO in the $NaC_2H_3O_2$/DIH_2O (red boxes and line, experimental and simulated circuit, respectively), KNO_3/DIH_2O (black circles and line, experimental and simulated circuit, respectively), and $NaNO_3$/DIH_2O (green triangles and line, experimental and simulated circuit, respectively) systems from 0.1 Hz to 10 KHz, as well as the equivalent circuit. Nyquist diagrams shows that in the 3 aqueous mediums, there is a diffusive process of the DAFCHO compound because it has a linearity of the impedance real with the imaginary impedance with an approximate angle of 45º. This results also indicates that the DAFCHO compound exhibits conductive behaviour.

On the other hand, the equivalent circuit that represents the electrochemical behaviour of the glass/DAFCHO in the three supporting electrolytes is integrate by the solution resistance (Rs) in series with the parallel arrangement of the polarization resistance (Rp) and a constant phase element (CPE). The values of Rs, Rp and CPE with the supporting electrolyte KNO_3 were: 9708.1Ω, 4.31×10^{7}Ω? and 1.5867×10^{-7} F, with the $NaNO_3$ were: 189.03Ω, 5.69×10^{6}Ω and 3.1357 $\times10^{-7}$ F, while with the $NaC_2H_3O_2$ were: 189.86Ω, 5.70×10^{6}Ω and 2.7584×10^{-7} F. Therefore, with Rp values, thickness of DAFCHO (l= 0.7mm) and the area (A= 0.16cm^2), the electrical resistivity ($\rho = Rp * A/l$) of DAFCHO in the three supporting electrolytes (KNO_3, $NaNO_3$ and $NaC_2H_3O_2$) were obtained: 9.85×10^{7}Ω-cm, 1.3×10^{7}Ω-cm y 1.303 $\times10^{7}$Ω-cm respectively. According to the typical resistivity of solid materials, these values are in intermediate levels of conductivity (10^{-3} to 10^{7}Ω-cm) (Singh, 2017), which corroborates that the DAFCHO compound is a semiconductor material.

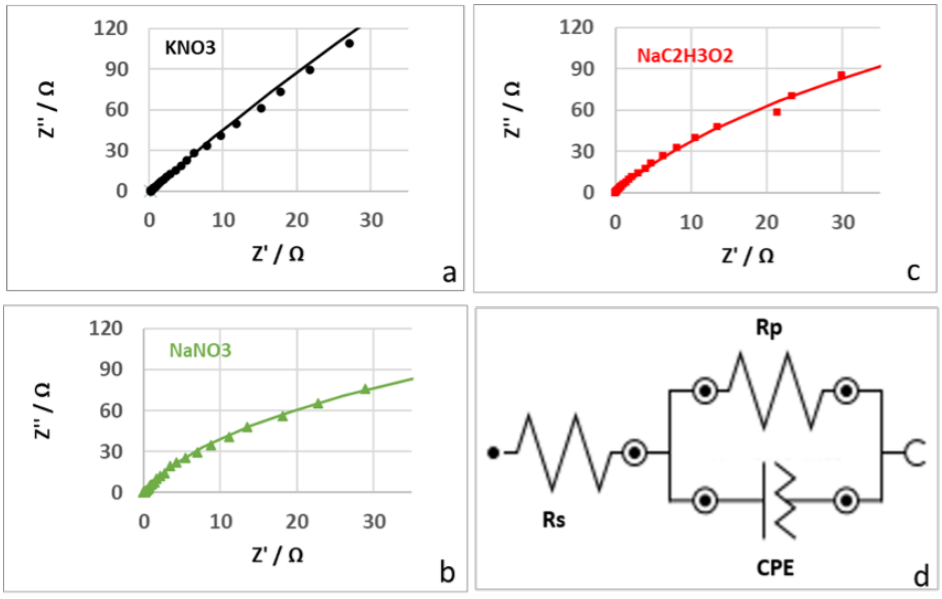

Fig. 6. Nyquist diagrams obtained on glass/DAFCHO in the a) KNO_3/DIH_2O (black circles and line, experimental and simulated circuit, respectively), b) $NaC_2H_3O_2$/DIH_2O (red boxes and line, experimental and simulated circuit, respectively), c) $NaNO_3$/DIH_2O (green triangles and line, experimental and simulated circuit, respectively) systems from 0.1 Hz to 10 KHz and d) equivalent circuit.

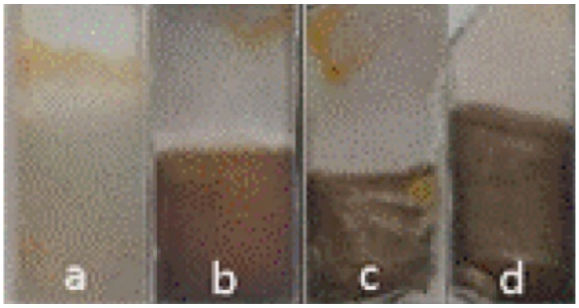

Fig. 7. Conjugated compound glass/ITO/DAFCHO films in different systems: (a) BU4NPF6-ACN, [(b) $NaC_2H_3O_2$, (c) KNO_3, (d) $NaNO_3$]-DIH_2O, after cyclic voltammetry at scanning speeds of 50 mVs^{-1} and 100 mVs^{-1}.

3.5 Surface degradation of glass/ITO/ DAFCHO

The electrochemical bandgap evaluation in various electrolytic medium revealed the film degradation of the conjugated compound DAFCHO. Figure 7 shows the film degradation images of the DAFCHO, after performing the CV at 50 and 100 mVs^{-1} in each of the supporting electrolytes under study. We observed that the organic film in the supporting electrolyte (a) BU_4NPF_6/ACN presented little degradation as there was less colour change in the film after the CV evaluations. While in the aqueous systems used as supporting electrolyte: (b) $NaC_2H_3O_2$/DIH_2O, (c) KNO_3/DIH_2O and (d) $NaNO_3$/DIH_2O, the organic material film presented a significant degradation. This, when observing a darkening in the films, caused by the rapid oxidation promoted by the interaction with the electrolytes, that were used to evaluate the DAFCHO electrochemical bandgap. Therefore, note that although the film structure of DAFCHO suffered a greater degradation when the CV was carried out in the $NaC_2H_3O_2$, KNO_3 and $NaNO_3$ electrolytic medium, the irreversible nature of the reactions allowed the evaluation of electrochemical bandgap $Eg_{(EC)}$ at 100 mVs^{-1} and 50 mVs^{-1}. Compared with the performance of DAFCHO in the BU_4NPF_6/ACN system, where a better surface stability was observed in the film with a bandgap value of 2.35 eV at 50 mVs^{-1} and of 2.61 eV at 100 mVs^{-1}.

3.6 X-ray diffraction (XRD) of glass/ITO/ DAFCHO

Figure 8 shows the XRD patterns obtained on the glass, glass/DAFCHO, glass/ITO/DAFCHO without electrochemical process, and glass/ITO/DAFCHO when was electrochemically degraded in the mediums used as supporting electrolytes: a) BU_4NPF_6/ACN, b) $NaC_2H_3O_2$/DIH_2O, c) KNO_3/DIH_2O and d) $NaNO_3$/DIH_2O.

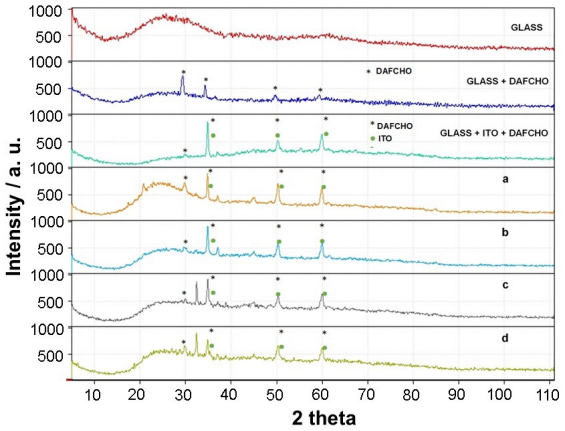

Fig. 8. XRD patterns obtained on the glass, glass/ DAFCHO and glass/ITO/DAFCHO without electrochemical process and glass/ITO/DAFCHO electrochemically degraded in: a) BU_4NPF_6/ACN, b) $NaC2H_3O_2$/DIH_2O, c) KNO_3/DIH_2O and d) $NaNO_3$/DIH_2O.

In the diffraction patterns a, b, c and d were observed the characteristic peaks of the ITO and the DAFCHO compounds. However, a quantity of amorphous material presents a crescent in the range of 20° to 30° in 2θ for glass/ITO/DAFCHO that was electrochemically degraded in BU_4NPF_6/ACN and aqueous mediums ($NaC_2H_3O_2$, KNO_3 and $NaNO_3$), similar to the diffraction pattern of glass when standing alone. While in diffraction patterns of GLASS+ITO+DAFCHO and GLASS+DAFCHO without an electrochemical process, a more homogeneous material can be seen in this interval (20° to 30° in 2θ). This behaviour was attributed to the fact that after the electrochemical process of glass/ITO/DAFCHO in the supporting electrolytes, the glass is exposed by the partial degradation of the ITO/DAFCHO film. Nevertheless, is important mention that the aqueous supporting electrolytes were only used to evaluate the electrochemical bandgap and did not interfere with the application of this compound, since it will not be subjected to these aqueous medium.

Conclusions

We found that it was possible to evaluate the electrochemical bandgap of the conjugated organic compound of oligophenylenimine (DAFCHO), deposited directly on a glass surface in the film form by using the self-assembly technique. Without the requirement of the conventional method where the organic material is deposited on an indium tin oxide-covered glass surface, it was possible to determine the electrochemical bandgap of the conjugated organic compound (glass/DAFCHO) in electrolytic aqueous medium ($NaC_2H_3O_2$, KNO_3 and $NaNO_3$)/DIH_2O) with values of 2.58 eV, 2.64 eV and 2.59 eV, at scanning speeds of 50 mVs^{-1} which were similar to those obtained with the optical bandgap in solution reported in the literature (2.56 eV) and the optical bandgap on glass/DAFCHO of this work (2.34 eV). Thus, the electrochemical bandgap calculation for the conjugate compound DAFCHO, evaluated in various electrolytic aqueous medium, indicated that this material had semiconductor characteristics (less than 3 eV, corresponding to the bandgap of organic semiconductors). In addition, this was evident in the evaluation of the current-voltage curve of the organic compound DAFCHO, which exhibited the characteristic behaviour of a P-N-type junction diode, with respect to low voltages. While that the electrochemical impedance measurements and electrical resistivity calculated indicates that the DAFCHO compound is a semiconductor material. Finally, we observed that even with a greater degradation of the organic compound film (glass/ITO/DAFCHO) in the aqueous systems: $NaC_2H_3O_2$/DIH_2O, KNO_3/DIH_2O and $NaNO_3$/DIH_2O, than that in the BU_4NPF_6/ACN system, it was possible to evaluate the electrochemical bandgap $Eg_{(EC)}$.

Acknowledgments

Amado Briseño Miguel Angel would like to thank PROMEP-UAEH for the funding received for the development of this research and CONACYT for postgraduate scholarship 588018. The authors are grateful to CONACYT for project 1227 of the Cátedras programme.

References

Abbas, Q., Gollas, B., & Presser, V. (2019). Reduced faradaic contributions and fast charging of nanoporous carbon electrodes in a concentrated sodium nitrate aqueous electrolyte for supercapacitors. *Energy Technology 7(9)*, 1-9. https://doi.org/10.1002/ente.201900430

Amado-Briseño, M. Á., Hernández-Ortíz, O. J., Rodríguez, M. A. V., Ayala, K. A., del Pozo Melero, G., Herrero, B. R., Zanabria, A. G. H., Roa, A. E., & Vázquez-García, R. A. (2022). Mechanosynthesis of 2,2?-((1E,1?E)-(2,5-bis(octyloxy)-1,4-phenylene)bis(ethene-2,1-diyl))bis(6-bromoquinoline): optical, electroluminescence, electrical, electrochemical, and morphological studies. *Journal of Materials Science: Materials in Electronics 33(1)*, 126-138. https://doi.org/10.1007/s10854-021-07271-w

Amado-Briseño, M. A., Zárate-Hernández, L. Á., Alemán-Ayala, K., Alonso, O. C., Cruz-Borbolla, J., Vásquez-Pérez, J. M., Reyes-Cruz, V. E., Veloz-Rodríguez, M. A., Rueda-Soriano, E., Pandiyan, T., & Vázquez-García, R. A. (2019). Mechanosynthesis of photochromic oligophenyleneimines: Optical, electrochemical and theoretical studies. *Molecules 24(5)*. https://doi.org/10.3390/molecules24050849

Arrieta-Almario, AA, Mendoza-Fandiño, JM, & Palencia-Luna, MS (2020). Material compuesto elaborado a partir de biopolímero conductor de almidón de yuca y polianilina. *Revista Mexicana de Ingeniería Química 19 (2)*, 707-715. https://doi.org/10.24275/rmiq/Mat765

Banerjee, M., Bhosle, A. A., Chatterjee, A., & Saha, S. (2021). Mechanochemical synthesis of organic dyes and fluorophores. *Journal of Organic Chemistry 86(20)*, 13911-13923. https://doi.org/10.1021/acs.joc.1c01540

Bernal, W., Anandhan, K., Percino, M. J., Barbosa-García, O., Pérez-Gutiérrez, E., Cerón, M., Maldonado, J. L., Rivadeneyra, M. S.,

& Thamotharan, S. (2021). Optoelectronic properties of (Z)-3-(4-(4,5-diphenyl-1H-imidazole-2-yl)phenyl)-2-phenylacrylonitrile films under acid and thermal environments for tuning OLED emission. *Dyes and Pigments 187*(January 2020), 1-10. https://doi.org/10.1016/j.dyepig.2020.109115

Chooto, P. (2019). Cyclic voltammetry and its applications. *Voltammetry*. https://doi.org/10.5772/intechopen.83451

Dinesh Pathak, Sanjay Kumar, Sonali Andotra, Jibin Thomas, Navneet Kaur, P. K. and V. K. (2021). New tailored organic semiconductors thin films for optoelectronic applications. *Physics of Organic Materials and Devices 95* (*Eur. Phys. J. Appl. Phys.*), 10.

Duan, L., & Uddin, A. (2020). Progress in stability of organic solar cells. *Advanced Science 7(11)*. https://doi.org/10.1002/advs.201903259

ensayos-mediante-uv-vis @ www.labte.es. (n.d.). http://www.labte.es/index.php/es/2013-11-03-19-54-23/tecnicas-espectroscopicas/ensayos-mediante-uv-vis

Espinosa-Roa, A., Cruz-Carrillo, M. de J., Ledesma-Juárez, A., Montoya del Angel, A., Romero-Borja, D., Güizado-Rodríguez, M., Rodríguez, M., Galindo, R., Maldonado, J. L., & Barba, V. (2019). Synthesis of polyfluorenes by oxidative polymerization, their characterization and implementation in organic solar cells. *Journal of Materials Science: Materials in Electronics 30(3)*, 2716-2725. https://doi.org/10.1007/s10854-018-0547-2

Flores-Noria, R., Vázquez, R., Arias, E., Moggio, I., Rodríguez, M., Ziolo, R. F., Rodríguez, O., Evans, D. R., & Liebig, C. (2014). Synthesis and optoelectronic properties of phenylenevinylenequinoline macromolecules. *New Journal of Chemistry 38(3)*, 974. https://doi.org/10.1039/c3nj01193c

Jia, X., Baird, E. C., Blochwitz-Nimoth, J., Reineke, S., Vandewal, K., & Spoltore, D. (2021). Selectively absorbing small-molecule solar cells for self-powered electrochromic windows. *Nano Energy 89(PB)*, 106404. https://doi.org/10.1016/j.nanoen.2021.106404

Ke, Y., Chen, J., Lin, G., Wang, S., Zhou, Y., Yin, J., Lee, P. S., & Long, Y. (2019). Smart windows: Electro-, thermo-, mechano-, photochromics, and beyond. *Advanced Energy Materials 9(39)*, 1-38. https://doi.org/10.1002/aenm.201902066

Li, H., Zhang, Y., Hu, Y., Ma, D., Wang, L., Jing, X., & Wang, F. (2004). *Novel Soluble N - Phenyl-Carbazole-Containing PPVs for Light-Emitting Devices?: Synthesis , Electrochemical, Optical, and Electroluminescent Properties*. 247-255. https://doi.org/10.1002/macp.200300037

Mejía-Hernández, F. G., Hernández-Ortíz, O. J., Muñoz-Pérez, F. M., Martínez-Pérez, A. I., Vázquez-García, R. A., Vera-Cárdenas, E. E., ... & Alemán-Ayala, K. (2021). Mechanochemical synthesis, linear and nonlinear optical properties of a new oligophenyleneimine with indole terminal moiety for optoelectronic application. *Journal of Materials Science: Materials in Electronics 32(5)*, 6283-6295. https://doi.org/10.1007/s10854-021-05344-4

Noirbent, G., Pigot, C., Bui, T. T., Péralta, S., Nechab, M., Gigmes, D., & Dumur, F. (2021). Dyes with tunable absorption properties from the visible to the near infrared range: 2,4,5,7-tetranitrofluorene (TNF) as a unique electron acceptor. *Dyes and Pigments, 189*(January). https://doi.org/10.1016/j.dyepig.2021.109250

Pérez, A. I. M., Alonso, O. C., Borbolla, J. C., Vásquez-Pérez, J. M., Alonso, J. C., Ayala, K. A., Luna-Bárcenas, G., Pandiyan, T., & García, R. A. V. (2015). Synthesis of photochromic oligophenylenimines: Optical and computational studies. *Molecules, 20(4)*, 5440-5455. https://doi.org/10.3390/molecules20045440

Rau, U., & Kirchartz, T. (2019). Charge carrier collection and contact selectivity in solar cells. *Advanced Materials Interfaces 6(20)*. https://doi.org/10.1002/admi.201900252

Saeed, Z. M., Dhokale, B., Shunnar, A. F., Awad, W. M., Hernandez, H. H., Naumov, P., & Mohamed, S. (2021). Crystal engineering of binary organic eutectics: Significant improvement in the physicochemical properties of polycyclic aromatic hydrocarbons via the

computational and mechanochemical discovery of composite materials. *Crystal Growth and Design 21(7)*, 4151-4161. https://doi.org/10.1021/acs.cgd.1c00420

Saive, R. (2019). S-shaped current-voltage characteristics in solar cells: A review. *IEEE Journal of Photovoltaics 9(6)*, 1477-1484. https://doi.org/10.1109/JPHOTOV.2019.2930409

Sandford, C., Edwards, M. A., Klunder, K. J., Hickey, D. P., Li, M., Barman, K., Sigman, M. S., White, H. S., & Minteer, S. D. (2019). A synthetic chemist?s guide to electroanalytical tools for studying reaction mechanisms. *Chemical Science 10(26)*, 6404-6422. https://doi.org/10.1039/c9sc01545k

Singh, V. (2017). Band gap and resistivity measurements of semiconductor materials for thin films. *Journal of Emerging Technologies and Innovative Research (JETIR) 4(12)*, 1200-1210. https://www.jetir.org/view?paper=JETIR1712169

Sweety, Vashistha, V. K., Kumar, A., & Singh, R. (2019). Synthesis, electrochemical and antimicrobial studies of me6-dibenzotetraazamacrocyclic complexes of Ni(II) and Cu(II) metal ions. *Russian Journal of Electrochemistry 55(3)*, 161-167. https://doi.org/10.1134/S1023193519020113

Vazquez, A., Rodriguez, M., Castro-Carranza, A., Martinez-Castillo, J., Maldonado, J. L., Gutowski, J., & Nolasco, J. C. (2020). Numerical simulation of a bilayer organic solar cell based on boron chromophore compounds as acceptors. *2020 IEEE International Conference on Engineering Veracruz, ICEV 2020*. https://doi.org/10.1109/ICEV50249.2020.9289666

xps @ www.scai.uma.es. (n.d.). https://www.scai.uma.es/areas/aqcm/xps/xps.html

Yahia, I. S., Zahran, H. Y., & Alamri, F. H. (2016). Pyronin y as new organic semiconductors: Structure, optical spectroscopy and electrical/dielectric properties. *Synthetic Metals 218*, 19-26. https://doi.org/10.1016/j.synthmet.2016.04.024